Contents

This page intentionally left blank

Good approximations often lead to better ones.

Mathematical Methods in Science
George Pòlya, 1977

Chapter 4

Calculation and modelling of subgrid tendencies

TODO: introductory paragraph: why am I doing this?

4.1 Calculation of subgrid tendencies

The workflow used to calculate the subgrid tendencies is described below and illustrated as a flowchart in Figure 4.1, which uses the same numbering to show the order of the steps.

1. The fine model was integrated for [TODO:] time units. Every 3 time units, the model state was saved, and then saved again one time step later. This resulted in a dataset of [TODO:] pairs of snapshots separated by 3 time units. An interval of 3 time units was chosen as it was the approximate decorrelation time of the model variables (see Appendix A.5); using a shorter interval would result in saving redundant information.

2. Each pair of snapshots was *coarse-grained*, reducing its spatial resolution to that of the coarse model. The nature of the coarse-graining operation warrants special attention and is discussed separately in § 4.2.

3. The first coarse-grained snapshot in each pair was input as an initial condition for the coarse model. The coarse model integrated for one time step only, and the resulting state—the coarse model's prediction for the large-scale state after one time step—was saved.

4. The first coarse-grained snapshot in each pair from Step 2 was subtracted from the second and the difference divided by the fine model's time step, giving the *true coarse tendency* (i.e., the true time derivative of the large-scale state as calculated by the fine model).

5. The first coarse-grained snapshot in each pair from Step 2 was subtracted from the coarse model prediction produced in Step 3 and the difference divided by the coarse model's time step, giving the tendency predicted by the coarse model (i.e., its prediction of the time derivative of the large-scale state).

6. Finally, the coarse model predicted tendencies from Step 5 were subtracted from the true coarse tendencies from Step 4, producing the *subgrid tendencies*. These measure the error in the coarse model's prediction of the time derivative of the large-scale state, and would be identically zero for a perfect coarse model.

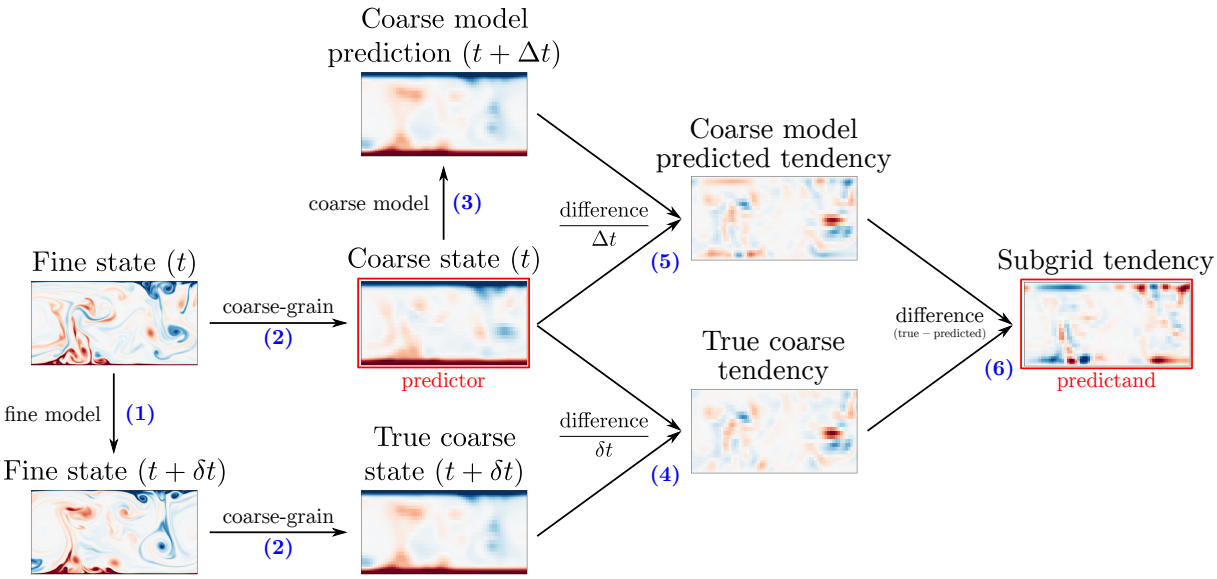

Figure 4.1: Flowchart illustrating the procedure used to calculate subgrid tendencies. The plots show an example of the workflow being applied to the temperature data but are for illustrative purposes only. The blue numbers correspond to the steps described in the text.

4.2 Choice of coarse-graining method

Coarse-graining is the process of reducing a gridded dataset onto a lower-resolution grid, and it is required at Step 2 of the workflow described in § 4.1. It was found that the choice of coarse-graining method was a major influence on the quality of the calculated subgrid tendencies; this is the consequence of a subtle issue that may seem purely semantic at first but in fact has important practical implications.

In general, the output of a coarse (i.e., reduced-order) model is meant to approximate a certain *representation* of the output of a chosen fine model. To give three concrete examples, the coarse model might seek to reproduce (a) the values of the high-resolution fields on a sparser grid of points, or (b) the averages over a set of larger grid boxes, or (c) the first N coefficients of the discrete Fourier transform (where N is less than the number of coefficients needed to fully determine the original fields). The modeller has the freedom choose a representation, which in turn determines how the output of the coarse model should be interpreted. The choice of representation also implicitly determines a coarse-graining operation: a map from the state space of the fine model to the state space of the coarse model that isolates the necessary large-scale information and discards the rest. Referring to the previous examples, option (a) calls for an operation that simply discards, say, three out of every four or nine out of ten grid points. Option (b) calls for the grouping and averaging of the grid points that lie within each large grid box. Option (c) calls for the truncation of fine fields at the Nth coefficient in Fourier space.

The key lesson that was learnt during the course of this work is that the chosen representation and coarse-graining method must be appropriate to the nature of the coarse model. In this work, the coarse model was a Dedalus solver that, in Step 3 of the workflow in § 4.1, received gridded initial condition data in real space and integrated the governing equations forward in time using the same numerical method as the fine model. This gave rise to two constraints on the coarse-graining method:

1. The coarse-grained initial condition must be well-resolved on the coarse model's grid. Numerical solution algorithms for PDEs assume (e.g., by approximating derivatives as finite differences) that the solution is well-resolved on the discrete model grid, and can become unstable or produce output marred by artefacts if this condition is not met.

2. The initial condition must respect physical constraints, namely the divergence-free condition (3.9)

and the boundary conditions (3.10)–(3.12). A numerical algorithm cannot be expected to behave predictably when presented with unphysical initial conditions.

During the development of this study, before the above requirements were known, coarse-graining was performed by averaging the fine grid points that lay within each coarse grid box (a method known within the Earth sciences as *first-order conservative remapping* because it preserves mean values; see Jones 1999). Figure `TODO: figure comparing coarse-graining methods`, illustrating the application of first-order conservative remapping to sample temperature data, demonstrates that the result is not very well-resolved on the coarse grid; in many places, adjacent grid points have sharp differences in temperature. First-order conservative remapping is also not guaranteed to preserve boundary values or the divergence-free nature of the velocity field. Consequently, the tendencies obtained from the coarse model in Step 5 of the workflow suffered from noise and numerical artefacts that propagated to the subgrid tendencies in Step 6. With the signal of interest obscured, it was impossible to model the subgrid tendencies as functions of the coarse state.

It was evident that the coarse-graining method needed to involve a smoothing operation of some kind. However, most conventional smoothing methods, such as Gaussian filtering, also fail to preserve the boundary and divergence-free conditions. The solution to this problem was to supply each snapshot of the fine model state as an initial condition to an appropriate system of PDEs, chosen so that the integration of the system would have a smoothing effect on the initial condition data. The key advantage of this approach is that the boundary and divergence-free conditions can be explicitly enforced.

The choice of PDEs to achieve this was inspired by classical Gaussian filtering. Recall that a Gaussian filter convolves input data with a filter kernel that takes the form of a Gaussian function, which also happens to be the Green's function for the heat equation $\partial\psi/\partial t = \nabla^2\psi$ in an *infinite* domain. It follows that heat equations of some form on the *finite* domain of the Rayleigh-Bénard problem (whose Greeen's functions are not Gaussian) will have a similar smoothing effect while preserving the required boundary conditions. The appropriate equation for smoothing the temperature field θ is therefore

$$\frac{\partial\theta}{\partial t} = \nabla^2\theta \tag{4.1}$$

on $[0,\Gamma]\times[0,1]$ with $\theta(z=0) = +1/2$, $\theta(z=1) = -1/2$ and $\theta(x=0) = \theta(x=\Gamma)$. It is tempting to propose an equation of the same form, $\partial\boldsymbol{u}/\partial t = \nabla^2\boldsymbol{u}$, for the velocity field, but its solution on the finite domain would not necessarily preserve $\boldsymbol{\nabla}\cdot\boldsymbol{u} = 0$. By analogy to the incompressible Navier-Stokes equations, it is necessary to introduce a "pressure" term $-\boldsymbol{\nabla}\pi$ on the right-hand side, with the additional field $\pi(x,z)$ giving an additional degree of freedom that allows one to impose $\boldsymbol{\nabla}\cdot\boldsymbol{u} = 0$ without over-determining the problem. The velocity field is thus smoothed by the equations

$$\frac{\partial\boldsymbol{u}}{\partial t} = -\boldsymbol{\nabla}\pi + \nabla^2\boldsymbol{u} \quad \text{and} \tag{4.2}$$

$$\boldsymbol{\nabla}\cdot\boldsymbol{u} = 0 \tag{4.3}$$

on $[0,\Gamma]\times[0,1]$ with $\boldsymbol{u}(z=0) = \boldsymbol{u}(z=1) = \boldsymbol{0}$ and $\boldsymbol{u}(x=0) = \boldsymbol{u}(x=\Gamma)$. The equations (4.1)–(4.3) were integrated numerically on the same grid as the fine model using a solver that was straightforwardly implemented in Dedalus.

Once the high-resolution data had been smoothed using the method described above, all that remained was to downsample the result to the resolution of the coarse model using linear interpolation `TODO: actually using change scales function in dedalus`. To summarise, the coarse-graining workflow is as follows:

1. Input a high-resolution snapshot as the initial condition for the solver of (4.1)–(4.3).
2. Integrate the solver for 10^{-3} time units (the duration that was found to produce the necessary amount of smoothing) in steps of 2×10^{-4} time units. `TODO: check values`
3. Downsample the final state to the resolution of the coarse model and save the result.

4. Reset the solver and return to Step 1 to coarse-grain the next high-resolution snapshot.

Figure TODO: figure comparing coarse-graining methods demonstrates that the improved coarse-graining method produces smooth results that are well-resolved on the coarse grid, in contrast to first-order conservative remapping.

4.3 Analysis of subgrid tendencies

4.4 Modelling of subgrid tendencies

Bibliography

Jones, P. W. (1999). "First- and second-order conservative remapping schemes for grids in spherical coordinates". *Mon. Weather Rev.* **127**(9). DOI: 10.1175/1520-0493(1999)127<2204:FASOCR>2.0.CO;2.